



OPEN ACCESS

EDITED BY

Dawei Wang,
RWTH Aachen University, Germany

REVIEWED BY

Fei Pan,
RWTH Aachen University, Germany
Guoqing Sun,
Soochow University, China

*CORRESPONDENCE

Shenyang Cao,
✉ csy060113@outlook.com

RECEIVED 09 June 2025

ACCEPTED 03 July 2025

PUBLISHED 29 July 2025

CITATION

Wang X, Cao S, Wu X and Mu Q (2025)
Investigating adhesion mechanisms in
warm-mix recycled asphalt: a multiscale
atomic force microscopy and molecular
dynamics approach.
Front. Built Environ. 11:1643779.
doi: 10.3389/fbuil.2025.1643779

COPYRIGHT

© 2025 Wang, Cao, Wu and Mu. This is an
open-access article distributed under the
terms of the [Creative Commons Attribution
License \(CC BY\)](#). The use, distribution or
reproduction in other forums is permitted,
provided the original author(s) and the
copyright owner(s) are credited and that the
original publication in this journal is cited, in
accordance with accepted academic practice.
No use, distribution or reproduction is
permitted which does not comply with
these terms.

Investigating adhesion mechanisms in warm-mix recycled asphalt: a multiscale atomic force microscopy and molecular dynamics approach

Xiaolin Wang¹, Shenyang Cao^{2,3*}, Xu Wu⁴ and Qianqian Mu⁵

¹Gansu Hengda Road and Bridge Engineering Co., Ltd., Lanzhou, Gansu, China, ²Gansu New Development Investment Group Co., Ltd., Lanzhou, Gansu, China, ³School of Civil Engineering, Lanzhou University of Science and Technology, Lanzhou, Gansu, China, ⁴School of Civil Engineering, Lanzhou Jiaotong University, Lanzhou, Gansu, China, ⁵School of Computer Science and Information Engineering, Xinjiang Agricultural University, Urumqi, Xinjiang, China

The adhesion properties between warm-mix recycled asphalt and aggregates are a key bottleneck limiting the application of warm-mix recycled asphalt. To investigate the effects of aging, warm mix agent, and rejuvenator on the adhesion properties of SBS-modified asphalt and aggregates, this study used atomic force microscopy (AFM) to examine the surface microstructure of asphalt and aggregates. The classical Johnson-Kendall-Roberts and Derjaguin-Muller-Toporov mechanical models were chosen to characterize the micromechanics of asphalt with aggregates, and the influence of aging effects, rejuvenator, and warm mix agents on the adhesion behavior at the asphalt-aggregate interface was explored using the Fowkes surface energy theory. Molecular dynamics (MD) methods were used to investigate the interaction energy between asphalt and aggregates, and the adhesion work between asphalt and aggregates at the molecular level was calculated. A one-dimensional linear equation between AFM and MD is proposed, and a cross-scale relationship between AFM and MD is established. The research findings indicate that the aging process increases the roughness and adhesion of the asphalt surface through the formation of polar groups, while rejuvenators and warm mix agents counteract these effects through component supplementation and crystallization. The adhesion properties of asphalt with limestone are much higher than the adhesion properties of asphalt with granite, which is the fruit of the combined effect of van der Waals and electrostatic forces. AFM and MD have a good univariate linear functional relationship, the decidability coefficient $R^2 > 0.9$. These findings provide foundational insights for optimizing asphalt-aggregate combinations in pavement engineering.

KEYWORDS

warm-mixed recycled asphalt, adhesion properties, atomic force microscopy, molecular dynamics, linear correlation

1 Introduction

Asphalt materials undergo progressive aging when exposed to multiple environmental and mechanical stressors, including oxidative conditions, thermal fluctuations, ultraviolet

radiation, and traffic loading. This degradation process leads to the deterioration of pavement performance, manifesting as surface cracking, raveling, and other distress modes (Zhang D. et al., 2022). The rehabilitation of aged pavements generates substantial quantities of reclaimed asphalt pavement (RAP) materials. Conventional disposal approaches, such as uncontrolled stockpiling or landfilling, present significant environmental challenges and represent inefficient utilization of valuable resources (Luan et al., 2022). Consequently, the development of sustainable RAP recycling technologies has become a critical focus in pavement engineering, aiming to simultaneously address resource conservation and environmental protection objectives.

The hot recycling technology has long been recognized as one of the effective means of fully recovering RAP. However, high temperatures can lead to the production of large amounts of harmful gases during the recycling process, which are not only harmful to people's health, but also pollute the environment. Thus, warm mix agent was created. Numerous studies have shown that warm mixes can reduce the production temperature of asphalt by 30°C–50°C, which can significantly reduce pollutant emissions (Pan et al., 2021; Wang et al., 2020). Warm mix recycled asphalt technology represents a significant advancement in sustainable pavement construction by effectively addressing environmental concerns and re-source conservation. The adhesion properties between warm mix recycled asphalt and aggregates are a key factor in ensuring the long-term stability of their asphalt mixtures (Ayazi et al., 2017; Abd El-Hakim et al., 2021; Mohammed and Ismael, 2021). Currently, warm mix recycled asphalt is limited in its application due to its multi-phase complexity, which leads to unclear adhesion mechanism with aggregates.

Currently, atomic force microscopy (AFM) and molecular dynamics (MD) methods are widely used for their ability to well characterize the adhesion behavior between asphalt and aggregate. Li et al. (2023) evaluated the micromorphology and adhesion properties of interfacial and noninterfacial regions in cold recycled asphalt mixes using AFM. Zhang et al. used AFM to investigate the relationship between asphalt chemical composition and micromechanics (Zhang E. et al., 2022). In addition, some scholars have used AFM to quantitatively characterize the adhesion between asphalt and aggregate, and the results show that asphalt microform and aggregate type are important factors affecting the adhesion between asphalt and aggregate (Zhang M. et al., 2024; Ma et al., 2024; Sun et al., 2024; Xie et al., 2023). In addition, some researchers have explored the adhesion mechanism between asphalt and aggregate from a molecular point of view. Cui et al. found a strong correlation between the adhesion properties obtained from MD simulations and AFM tests (Cui et al., 2022). Sun et al. (2025), Yu et al. (2024) used MD to investigate the effect of aggregate mineral composition on the adhesion properties of asphalt and aggregate. The above studies have shown that the adhesion properties between asphalt and aggregate can be effectively evaluated using AFM and MD. Therefore, this paper was able to evaluate the effects of aging effects, rejuvenators and warm mixes on the adhesion properties of asphalt and aggregates using AFM and MD.

In this study, to investigate the effect of aging effect, rejuvenator and warm mix agent on the adhesion properties between SBS modified asphalt and aggregate, AFM test and molecular dynamics

TABLE 1 Physical indicators of SBS-modified asphalt.

Test items	Requirement value	Test value
Penetration (25°C, 100 g, 5 s)/0.1 mm	≥50	76
Ductility 5°C, 5 cm/min	≥35	45
Softening point (R&B)/°C	≥75	80.8
Dynamic viscosity 135°C/Pa·s	≤3	2.103

simulation were used in this paper to explore the adhesion properties between asphalt and aggregate. The adhesion force between asphalt and aggregate was tested separately using AFM and the adhesion work between asphalt and aggregate was calculated based on contact mechanics. The interaction energy and adhesion work between asphalt and aggregate were calculated using molecular dynamics method. A linear relationship between the two scales was established. The results of the study will be important for the application of warm mix recycled asphalt.

2 Materials and methods

2.1 Materials

2.1.1 SBS modified asphalt

The basic properties of SBS modified asphalt are shown in Table 1, and the SBS modifier content is 4.7% of the asphalt mass.

2.1.2 Rejuvenator

The basic physical properties of the rejuvenator are shown in Table 2. The rejuvenator consists of a vegetable oil, viscosity builder, and plasticizer. The content of the rejuvenator in the recycled asphalt binder was established at 10 wt%.

2.1.3 Warm-mix agent

The basic physical properties of the WMA are shown in Table 3. The WMA content is 3 wt% of the mass of asphalt.

2.1.4 Aggregate

In this experimental investigation, two distinct categories of mineral aggregates specifically, alkaline limestone and acidic granite—were carefully selected as representative specimens to systematically examine the influence of aggregate mineralogy on interfacial adhesion characteristics within asphalt-aggregate systems.

2.1.5 Preparation of asphalt samples

2.1.5.1 Preparation of aged SBS modified asphalt

Considering the limitations of the test conditions, this paper used the 270 min RTFOT (AASHTO, 2024) to simulate the long-term aging of asphalt, which has been proven to be feasible (Zhang M. et al., 2024).

2.1.5.2 Preparation of warm mixed recycled SBS modified asphalt binder

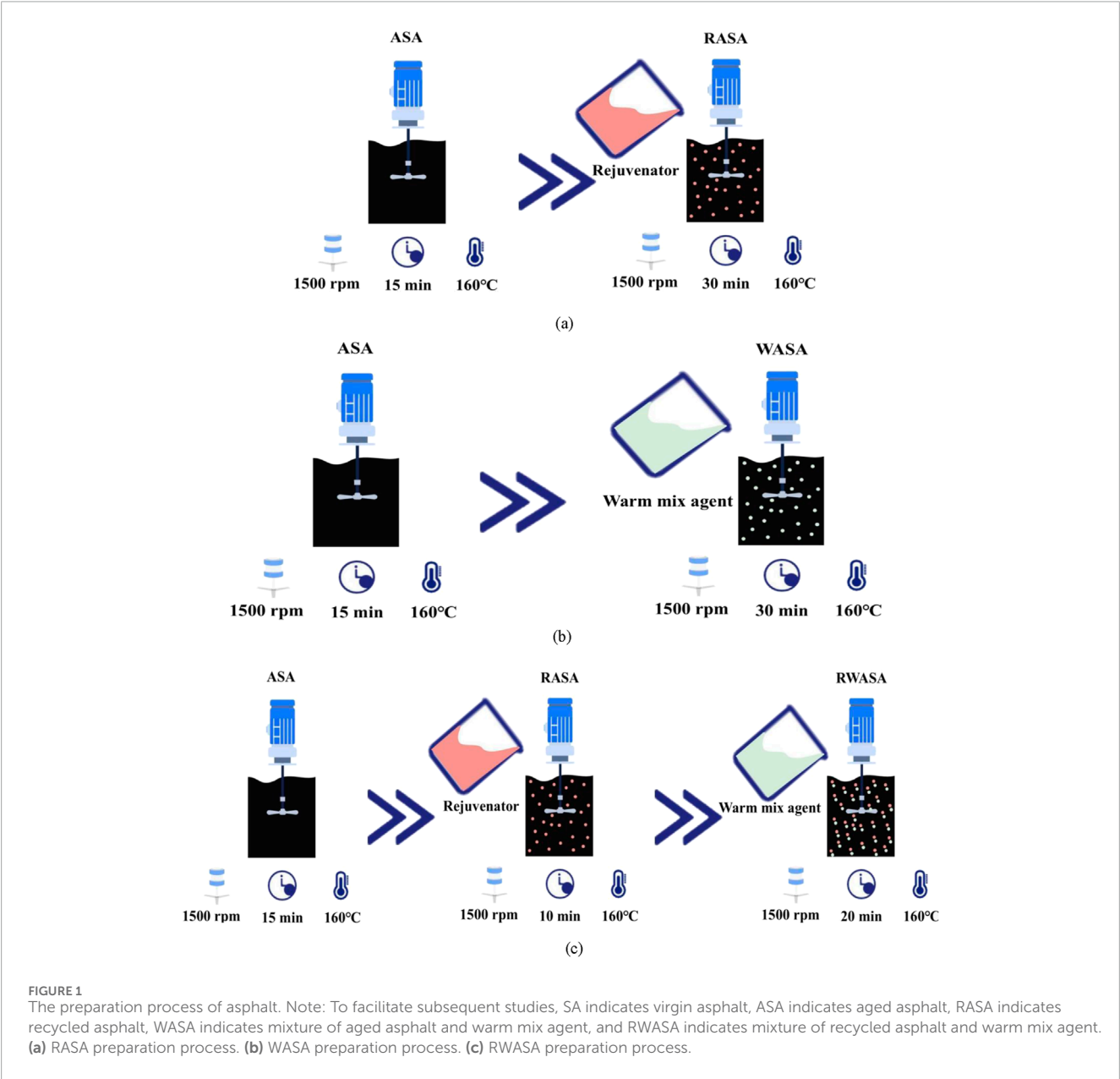
The preparation process of asphalt is shown in Figure 1.

TABLE 2 Physical indicators of rejuvenator.

Experiment	Viscosity (60°C)	Density	Flash point	Saturates	Aromatics	Loss in mass
	Pa·s	g/cm ³	°C	%	%	%
Measured value	112	0.948	213	36.5	26.6	2.150

TABLE 3 Physical indicators of WMA.

Appearance	Viscosity (Pa·s)	Density (g/cm ³)	Optimal content (%)
Milky white particles	12.2 × 10 ⁻³	0.96	3



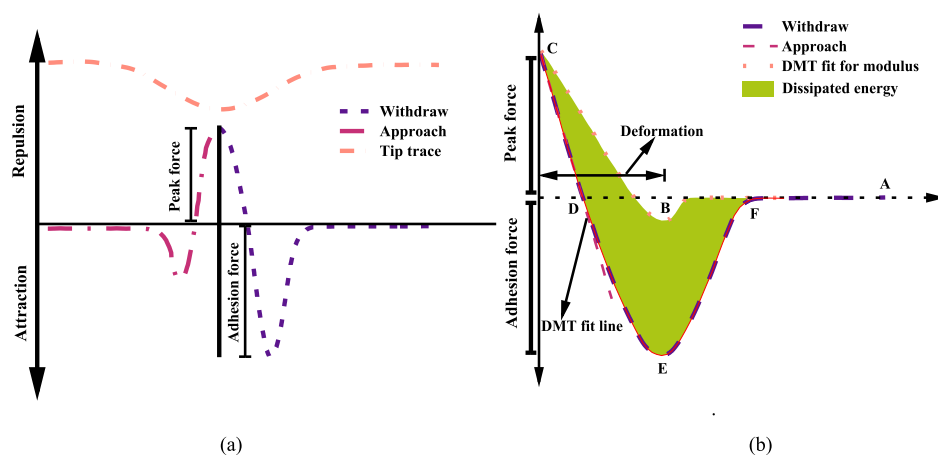


FIGURE 2
Schematic diagram of force profile and typical force profile. **(a)** Schematic diagram of force profile. **(b)** Typical force profile.

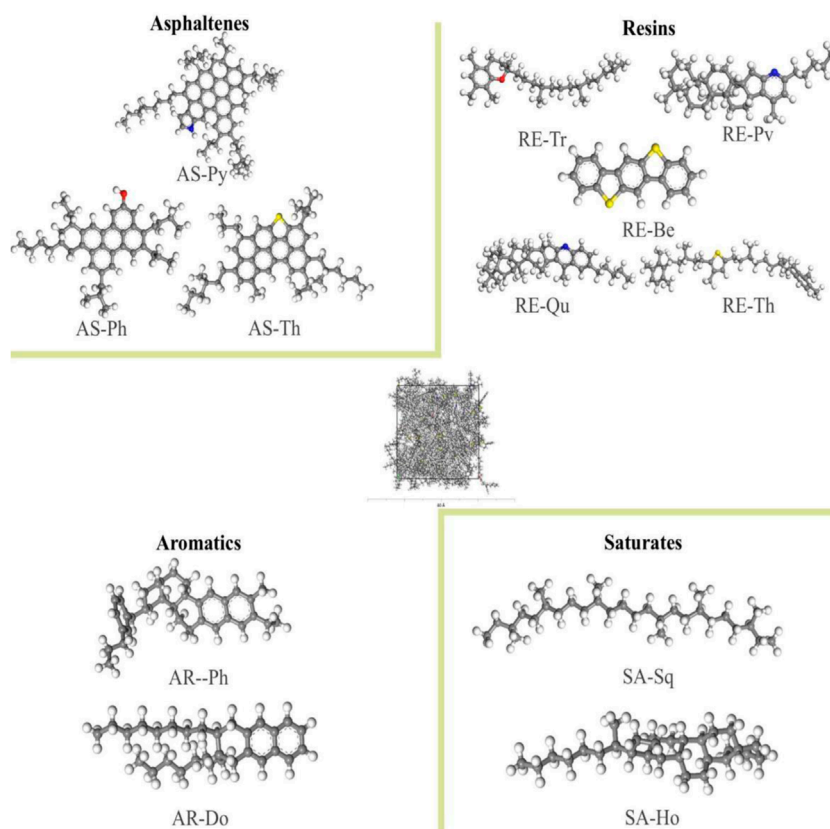


FIGURE 3
12-component molecular of virgin asphalt.

2.2 Test methods

2.2.1 Atomic force microscopy (AFM) test

2.2.1.1 AFM test for asphalt binder

The surface topography and nanomechanical properties of bituminous materials were characterized using atomic force

microscopy (Bruker Dimension Icon AFM) to investigate micro structural features and interfacial interactions at the nanoscale. The AFM analysis employed a dual-mode approach: 1) light-tapping mode for high-resolution topographic imaging and 2) contact mode for quantitative force measurements. All experiments were conducted under strictly controlled conditions, maintaining an

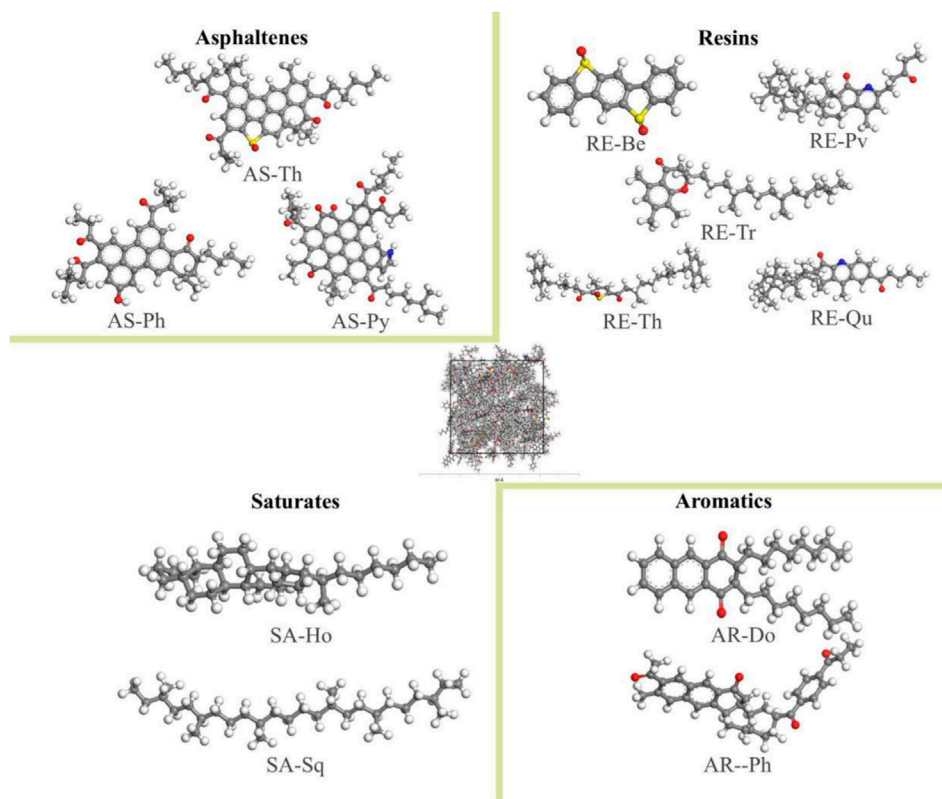


FIGURE 4
12-component molecular of aged asphalt.

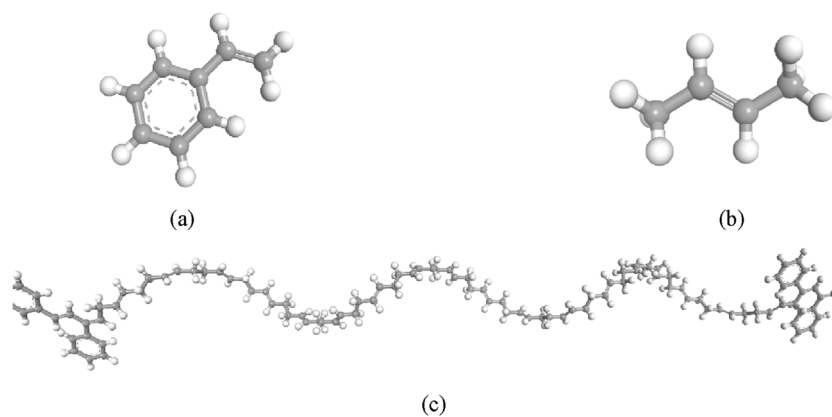


FIGURE 5
Molecular modeling of SBS modifiers. (a) Styrene. (b) Butadiene. (c) SBS.

ambient 25°C ($\pm 0.5^\circ\text{C}$). The scanning parameters included a $10 \times 10 \mu\text{m}^2$ analysis area, 2 Hz scan rate, and 256×256 pixel resolution, ensuring consistent measurement conditions across all specimens. A calibrated RFESPA-75 silicon probe (nominal tip radius = 8 nm, spring constant = 3 N/m) was used for all measurements, with each sample undergoing triplicate testing to ensure data reproducibility.

2.2.1.2 AFM test for aggregate

The nanoscale characterization of aggregate surfaces was performed using a Bruker Dimension Icon atomic force microscopy (AFM) following standardized analytical protocols. To ensure optimal resolution of surface features, the scanning area was reduced to $5 \times 5 \mu\text{m}^2$ compared to asphalt specimens, while maintaining identical environmental conditions. Prior to AFM

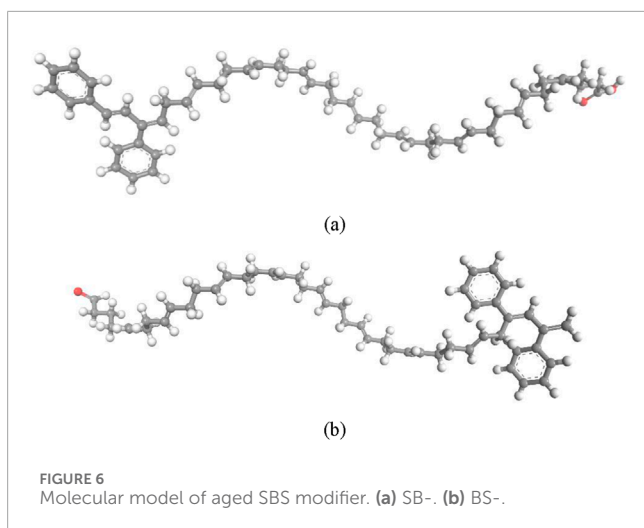


FIGURE 6
Molecular model of aged SBS modifier. (a) SB-. (b) BS-.

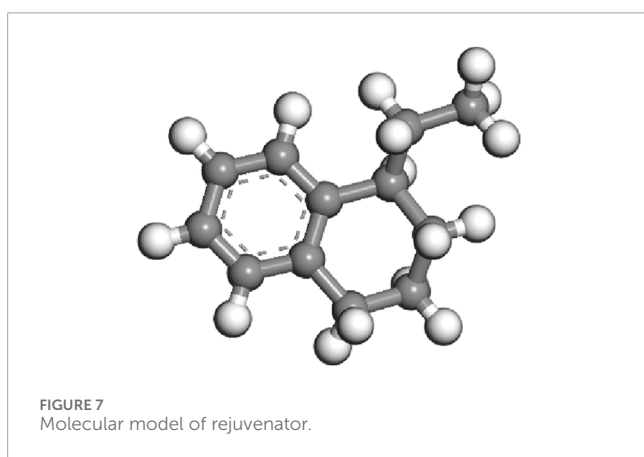


FIGURE 7
Molecular model of rejuvenator.

analysis, aggregate surfaces underwent precision polishing to achieve a surface roughness below 5 μm , a critical preparation step for obtaining reliable micro structural and force interaction data.

2.2.1.3 Evaluation of asphalt-aggregate micro-adhesion force

The adhesion characteristics at the asphalt-aggregate interface were quantitatively assessed through analysis of force-distance measurements, with representative profiles displayed in Figure 2a and typical interaction curves shown in Figure 2b. These experimental data were interpreted using two complementary theoretical frameworks from contact mechanics: the Johnson-Kendall-Roberts (JKR) formulation Equation 1 (Zhang Z. et al., 2024), appropriate for describing interactions with deformable asphalt surfaces, and the Derjaguin-Muller-Toporov (DMT) approach Equation 2 (Chen et al., 2021), more suitable for modeling contacts with rigid mineral substrates.

$$W_{as-p} = \frac{2}{3} \cdot \frac{F_{as-p}}{\pi R_{as-p}} \quad (1)$$

$$W_{ag-p} = \frac{1}{2} \cdot \frac{F_{ag-p}}{\pi R_{ag-p}} \quad (2)$$

Where, W_{as-p} and W_{ag-p} are the asphalt-probe and aggregate-probe adhesion work, respectively. F_{as-p} and F_{ag-p} are the asphalt-probe and aggregate-probe adhesion force, respectively, and the value corresponds to the lowest point in the withdrawal curve (see point E in Figure 2b). R_{as-p} and R_{ag-p} are the probe-asphalt contact area and probe-aggregate contact area, respectively, $R_{as-p} = R_{ag-p} = 8 \text{ nm}$. The interfacial bonding capacity between asphalt binder and mineral aggregate can be quantitatively assessed through Fowkes' surface energy theory, with the corresponding adhesion work calculations expressed in the following theoretical framework (Equations 3–5):

$$\gamma_{as} = \frac{W_{as-p}^2}{4\gamma_p} \quad (3)$$

$$\gamma_{ag} = \frac{W_{ag-p}^2}{4\gamma_p} \quad (4)$$

$$W_{as-ag} = 2\sqrt{\gamma_{as}\gamma_{ag}} \quad (5)$$

Where, γ_{as} is the surface free energy of the asphalt binder. γ_{ag} is the surface free energy of the aggregate. γ_p is the surface free energy of the silica probe, and γ_p is 38,213 mJ/m^2 . W_{as-ag} is the adhesion work between the asphalt and aggregate.

2.2.2 Molecular dynamics (MD) simulation

2.2.2.1 Virgin asphalt molecular

In this paper, the 12 components proposed by Li and Greenfield were used as the molecular model of virgin asphalt, as shown in Figure 3 (Li and Greenfield, 2014). The AAA-1 model represents the molecular model of asphalt (Ji et al., 2023).

2.2.2.2 Aged asphalt molecular

Aged asphalt contains a large number of oxygenated polar functional groups ($\text{C}=\text{O}$ and $\text{S}=\text{O}$) (Chen et al., 2021). The molecular model of aged asphalt used in this paper is shown in Figure 4 (Ding et al., 2021).

2.2.2.3 SBS molecular

SBS is a block copolymer with a specific ratio of styrene and butadiene monomers. The SBS modifier molecular model used in this paper is composed of 2 styrene, 18 butadiene, and 2 styrene as shown in Figure 5.

It was shown that the aging products of SBS are SB- and BS- obtained by oxidative breakage of double bonds, as shown in Figure 6 (Yu et al., 2023a).

2.2.2.4 Rejuvenator molecular

The chemical composition of the rejuvenator employed in this investigation was characterized by a specific molecular configuration, as illustrated in Figure 7, featuring a hydrocarbon structure with the molecular formula $\text{C}_{12}\text{H}_{16}$. This molecule has been shown to represent asphalt rejuvenator well.

2.2.2.5 Construction of asphalt molecular model

This paper utilized the amorphous cell module of MS software to construct molecular models of asphalt based on the number of molecules listed in Tables 4 (Wang et al., 2022; Qu et al.,

TABLE 4 Number of molecules in the different asphalt.

Molecular		Chemical formula	SA	ASA	RASA	WASA	RWASA
			Number of molecules				
Asphaltene	PH	C ₄₂ H ₅₄ O	3	5	5	5	5
	PY	C ₆₆ H ₈₁ N	2	4	4	4	4
	TH	C ₅₁ H ₆₂ S	3	5	5	5	5
Resin	BE	C ₁₈ H ₁₀ S ₂	15	18	18	18	18
	PV	C ₃₆ H ₅₇ N	4	6	6	6	6
	TR	C ₂₉ H ₅₀ O	5	7	7	7	7
	TH	C ₄₀ H ₆₀ S	4	6	6	6	6
	QU	C ₄₀ H ₅₉ N	4	6	6	6	6
Aromatic	DO	C ₃₀ H ₄₆	18	10	10	10	10
	PH	C ₃₅ H ₄₄	15	9	9	9	9
Saturate	HO	C ₂₉ H ₅₀	5	5	5	5	5
	SQ	C ₃₀ H ₆₂	4	4	4	4	4
SBS		C ₁₀₄ H ₁₃₄	4	-	-	-	-
SB-		C ₅₂ H ₆₆ O	-	4	4	4	4
BS-		C ₅₂ H ₆₆ O ₂	-	4	4	4	4
Rejuvenator		C ₁₂ H ₁₆	-	-	31	-	1
warm mix agent		C ₁₁ H ₂₄	-	-	-	9	9

2018). The number of SBS, rejuvenator, and warm mix agent molecules were determined by calculation to be 4, 31, and 9, respectively.

The molecular models of SA, ASA, RASA, WASA, and RWASA were built based on the number of molecules in each asphalt model in Table 3. The initial density of the asphalt molecular model was set to 0.8 g/cm³ to reduce the cross overlap between asphalt molecular chains. The molecular dynamics simulation flow of this study is shown in Figure 8.

2.2.2.6 Construction of the asphalt-aggregate interface molecular model

In this study, SiO₂ and CaCO₃ were chosen to represent common granite aggregates and limestone aggregates, respectively. The crystal models of SiO₂ and CaCO₃ are shown in Table 5.

To create orthogonal aggregate layers, γ in the SiO₂ and CaCO₃ crystal models must be transformed to 90°. In this paper, the [0, 0, 1] crystal facets of the SiO₂ model and the [1, 0, 4] crystal facets of the CaCO₃ model were selected for the granite aggregate model and the limestone aggregate model. It is important to note that after the SiO₂ is cleaved, the model needs to be saturated by adding “H” or “-OH”. Finally, the aggregate layer model is obtained by

expanding the cell. The construction process of the aggregate layer is illustrated in Figure 9.

The interface models between SA, ASA, RASA, WASA, and, RWASA with the aggregates were established by using the “Build Layers” function in MS software, as shown in Figures 10, 11.

2.2.2.7 Simulation methodology

Molecular dynamics simulations were conducted using Materials Studio 2021 software to investigate the interfacial interactions in the study. The computational analysis employed the COMPASS II force field (Han et al., 2024), which has been widely recognized for its reliability in modeling complex material systems. All simulations were performed in the NVT ensemble with the following parameters: 1) a total simulation time of 1000 picoseconds, including 500 ps for system equilibration; 2) constant temperature maintenance at 298 K using the Nose-Hoover thermostat method; 3) periodic boundary conditions applied in three dimensions.

2.2.2.8 Evaluation indicators

2.2.2.8.1 Interaction energy The interfacial interaction energy (E_i) serves as a fundamental thermodynamic parameter for evaluating the adhesive strength between dissimilar materials,

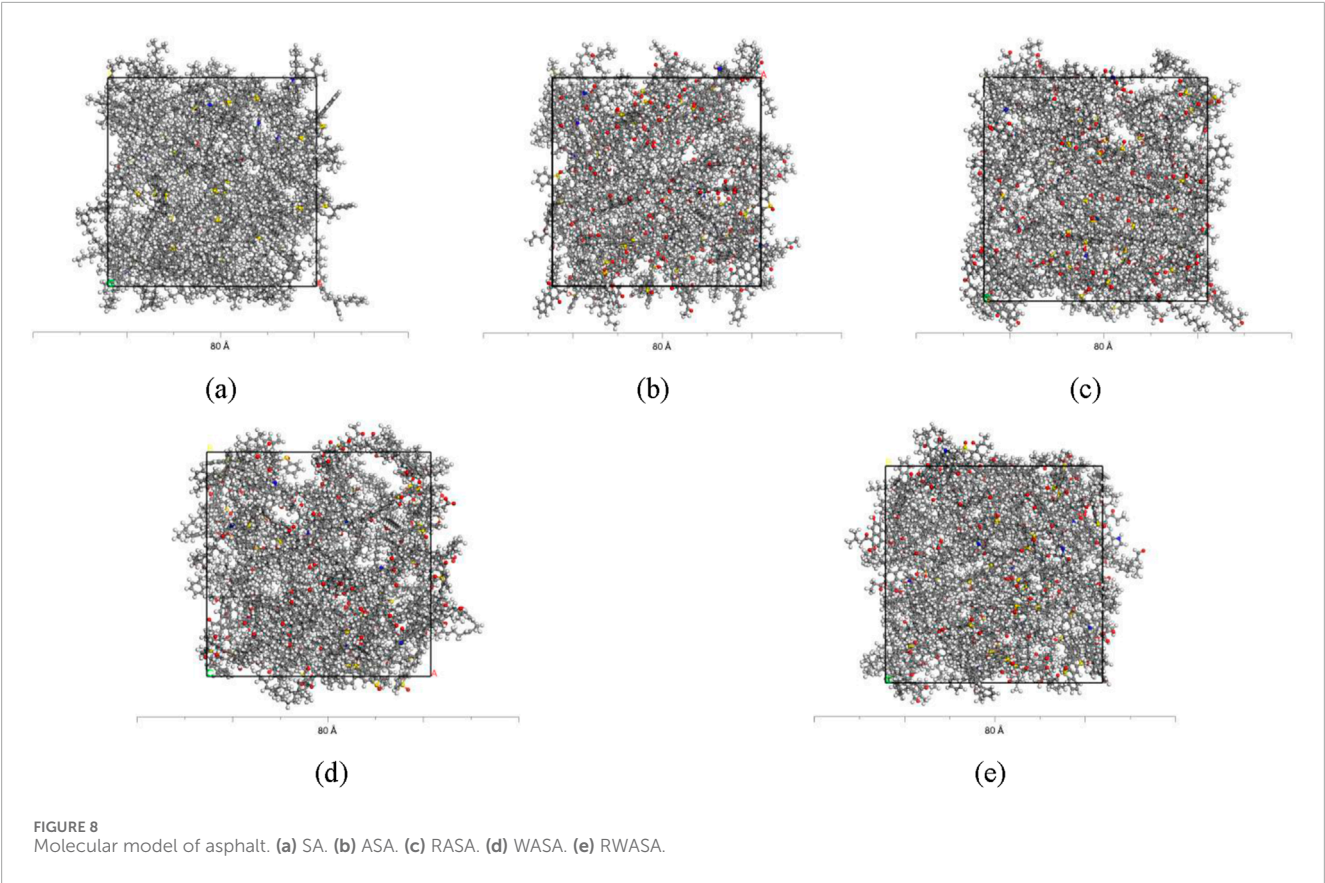
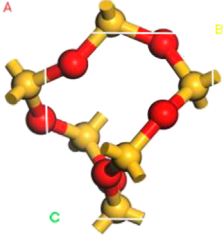
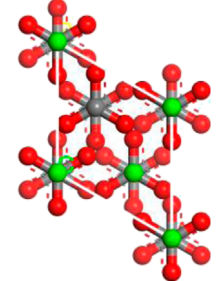


TABLE 5 Crystal parameters of SiO₂ and CaCO₃.

Crystal model	Chemical formula	Lattice parameters	Space group
	SiO ₂	a = b = 4.913 Å c = 5.4052 Å	α = β = 90° γ = 120°
	CaCO ₃	a = b = 4.99 Å c = 17.061 Å	α = β = 90° γ = 120°

representing the work required to separate two substances at their interface. This energy metric directly correlates with the fracture resistance and debonding behavior of material interfaces. In the current investigation, E_i was employed as a quantitative indicator of the bonding characteristics between asphalt binders and aggregate surfaces. The computational determination of E_i

followed established methodology (Gao et al., 2025), with the specific calculation expressed by Equation 6:

$$E_i = E_{Aggregate} + E_{AS} - E_{Aggregate+AS} \tag{6}$$

Where, E_i is the interaction energy between asphalt and aggregate, $E_{Aggregate}$ is the potential energy of the aggregate, E_{AS} is the potential

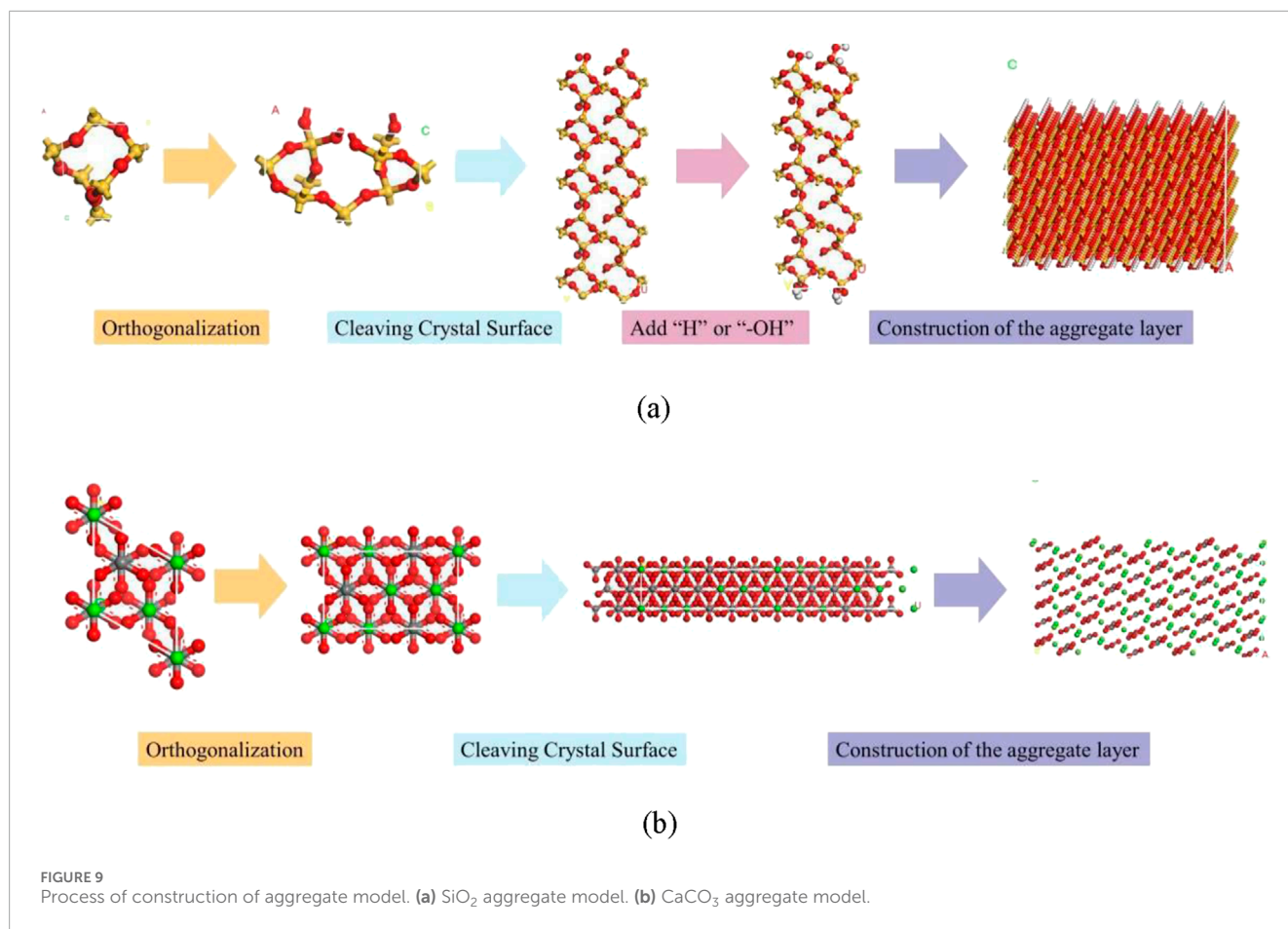


FIGURE 9
Process of construction of aggregate model. (a) SiO₂ aggregate model. (b) CaCO₃ aggregate model.

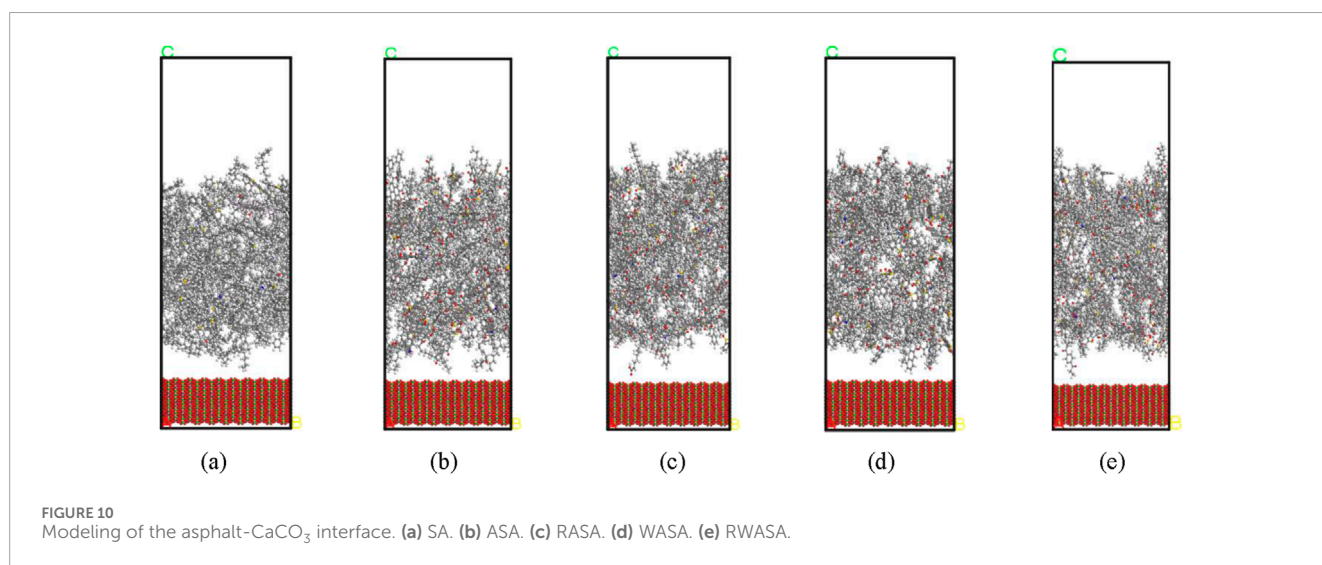


FIGURE 10
Modeling of the asphalt-CaCO₃ interface. (a) SA. (b) ASA. (c) RASA. (d) WASA. (e) RWASA.

energy of the asphalt; $E_{\text{Aggregate+AS}}$ is the potential energy at the interface of the asphalt and the aggregate.

2.2.2.8.2 Adhesion work. To alleviate the effect of interfacial dimensions on the adhesion at the asphalt-aggregate interface (Gao et al., 2025), this paper utilizes the adhesion work (W_{ag}), as

shown in Equation 7) to evaluate the adhesion performance between asphalt and aggregate (Guo F. et al., 2023).

$$W_{ta} = -\frac{E_i}{A} \quad (7)$$

Where, A is the contact area between the asphalt and the aggregate.

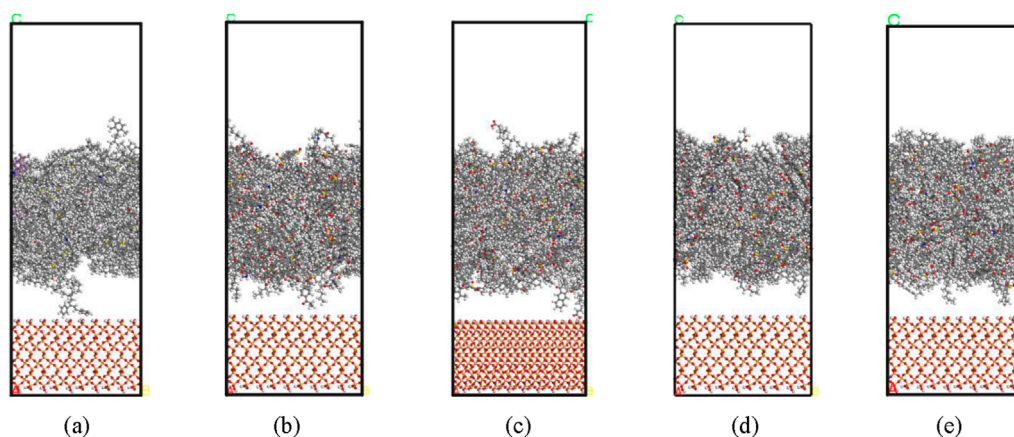


FIGURE 11
Modeling of the asphalt-SiO₂ interface. (a) SA. (b) ASA. (c) RASA. (d) WASA. (e) RWASA.

3 Results and discussion

3.1 AFM results analysis

3.1.1 Asphalt surface micro-morphology and micro-mechanics

3.1.1.1 Micro-morphological analysis of asphalt

To investigate the effect of aging, rejuvenator and warm mix agent on the surface micro-morphology of asphalt, this paper used AFM to test the surface morphology of SA, ASA, RASA, WASA, and, RWASA, as shown in Figure 12. Figure 12 shows the 3D microscopic morphology of SA, ASA, RASA, WASA, and, RWASA, respectively.

The 3D microscopic morphology of the aged asphalt ASA is shown in Figure 12b. The number of peaks in the ASA is significantly increased compared to the virgin asphalt SA. This substantial morphological alteration indicates a greater abundance and larger dimensions of columnar structures in ASA, primarily resulting from the accumulation of polar molecules during the aging process. The enhanced molecular aggregation can be attributed to two key factors: 1) the increased quantity of polar molecules in aged asphalt, and 2) the elevated polarity of SBS molecules following polymer degradation, which intensifies intermolecular interactions (Yu et al., 2023b). This is attributed to the fact that the degradation of SBS increases the number of oxygen-containing groups at its termini, which increases the polarity of the molecule. These findings corroborate existing research on asphalt aging mechanisms (Chen et al., 2018; Hu et al., 2022; Hu et al., 2023).

The introduction of rejuvenator produces notable changes in the asphalt morphology, as evidenced in Figure 12c. The treatment effectively reduces both the density of columnar structures and their peak heights, a phenomenon explained by the replenishment of light components and consequent decrease in relative polar component concentration (Pahlavan et al., 2022). When warm mix asphalt WASA additives are incorporated, the surface morphology undergoes further transformation, developing larger and more irregularly distributed needle-like crystalline structures (Figures 12d,e). This distinctive pattern arises from the presence of wax components in the WASA formulation, which

promotes the sedimentation and adhesion of various substances (including RE, SA, and AR) onto the surface of raw asphalt RWASA, ultimately forming characteristic “island” structures.

3.1.1.2 Micromechanical analysis of asphalt

To investigate the effect of rejuvenator and warm mix agent on the adhesion force between asphalt and probe, the force-curves test of AFM was used in this paper to obtain the withdrawal curve and approach curve between asphalt and probe, respectively, as shown in Figure 13.

From Figure 13b, it is found that the adhesion force between the aged asphalt and the probe is significantly higher than the adhesion force between the virgin asphalt and the probe. Compared to the virgin asphalt, the adhesion force between the aged asphalt and the probe increased by 49.96 nN. The results indicate that the aging effect increased the microscopic adhesion force between the SBS-modified asphalt and the silicon probe. This is mainly due to the aging of SBS and asphalt matrix to form a large number of polar functional groups, these polar functional groups are able to form hydrogen bonding interactions or acid-base interactions with the hydroxyl groups in SiO₂, thus increasing the adhesion between the SBS modified asphalt and the probe. This is mainly due to the fact that asphalt generates oxygenated polar groups that are acidic upon aging. The silica hydroxyl groups on the surface of SiO₂, on the other hand, are weakly basic. The adhesion between SiO₂ and asphalt is enhanced by acid-base interaction. Furthermore, after aging of SBS-modified asphalt, components such as asphaltene and resin aggregated on the surface of the asphalt and interacted strongly with SiO₂, thus enhancing the adhesion between the asphalt and the silicon probe. Compared to ASA, the adhesion force between RASA and silicon probe was reduced by 22.45 nN, as shown in Figure 13c. This means that the incorporation of regenerator weakened the adhesion force between aged SBS-modified asphalt and silicon probe. This is mainly attributed to the fact that the rejuvenator replenishes the lighter components of the aged asphalt and reduces the relative content of the polar components, weakening the interaction between the asphalt and the silica probes. The warm mix agent was able to weaken the

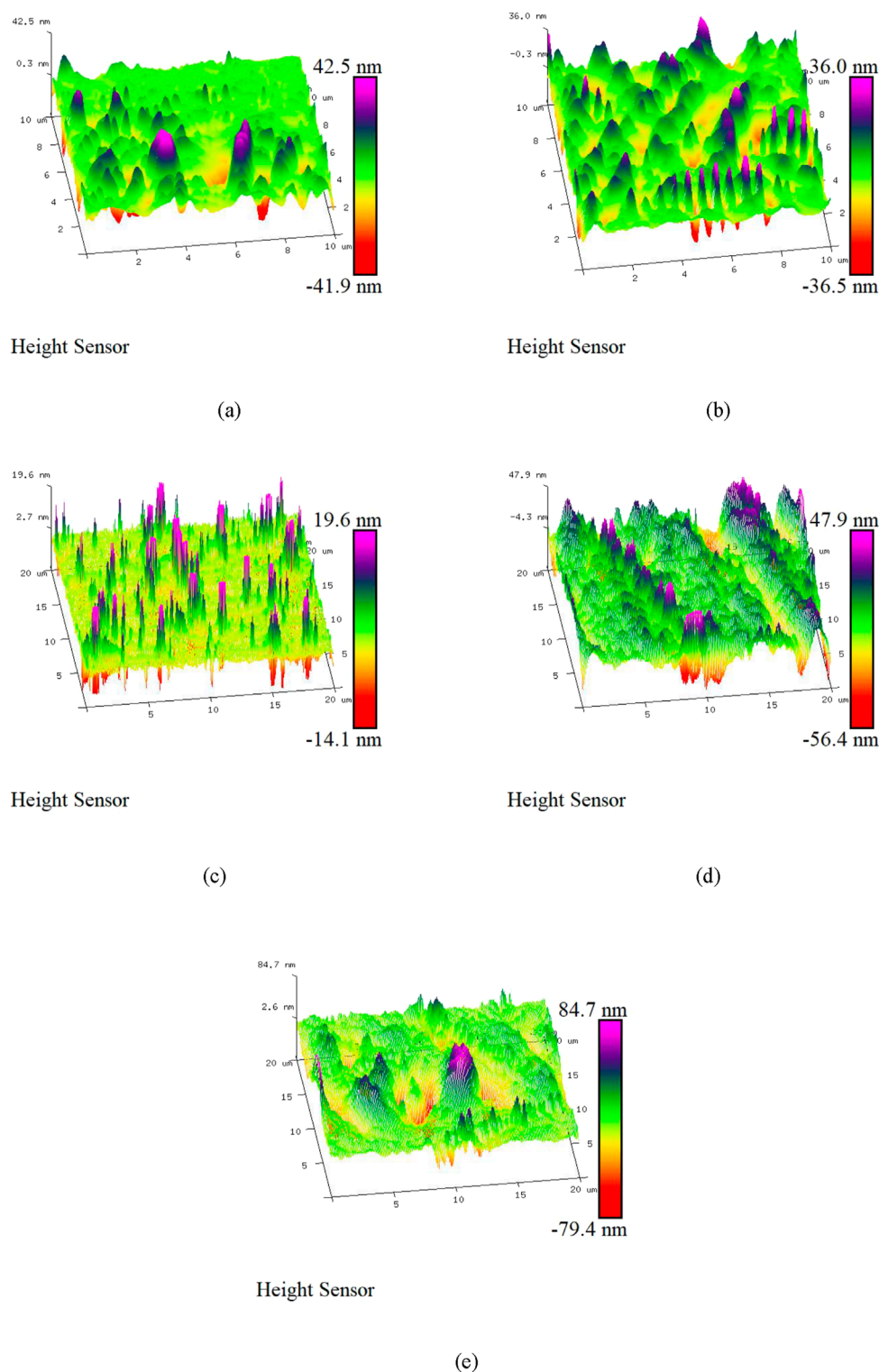


FIGURE 12
3D surface topography of asphalt binders. (a) SA. (b) ASA. (c) RASA. (d) WASA. (e) RWASA.

adhesion force between the aged SBS-modified asphalt and the probe, as shown in Figure 13d. Compared to ASA, the adhesion force between WASA and silicon probe was reduced by 11.27 nN. The results showed that the warm mix agent was able to reduce

the adhesion between the asphalt and the probe. This may be due to the fact that the warm mix crystallises at room temperature and inhibits the interaction between the polar functional groups in the bitumen and the silica, which reduces the adhesion between

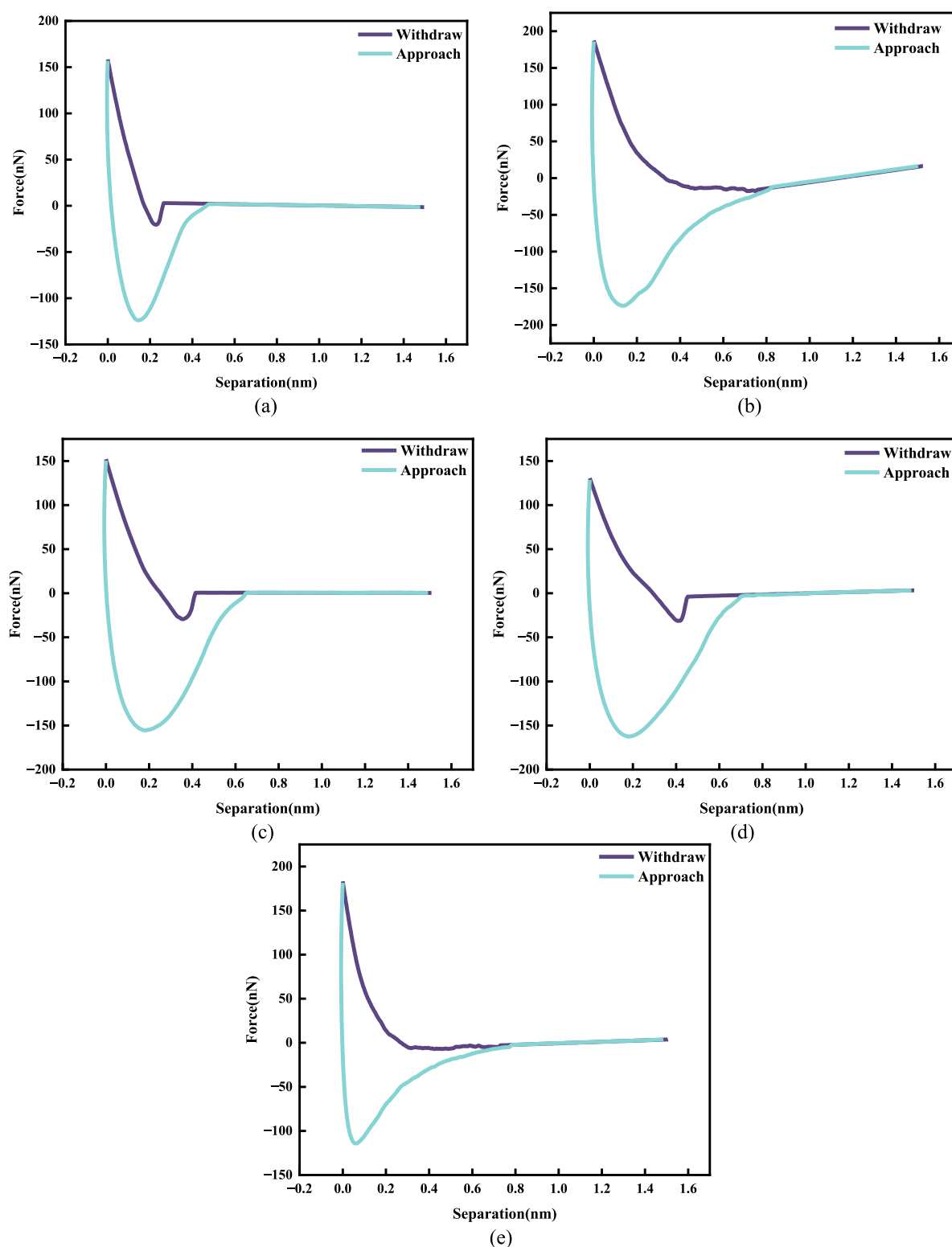


FIGURE 13
Force-curve diagram for different asphalt: (a) SA. (b) ASA. (c) RASA. (d) WASA. (e) RWASA.

the aged SBS modified asphalt and the silica probe. The adhesion force between the RWASA and the silicon probe was drastically reduced, as shown in Figure 13e. Compared to ASA, the adhesion force between RWASA and silicon probe was significantly reduced

by 59.88 nN. There are two main reasons for this phenomenon, one of which is that the rejuvenator dilutes the concentration of the polar component of the aged asphalt, weakening the interaction force between the polar component of the asphalt and the silicon probe.

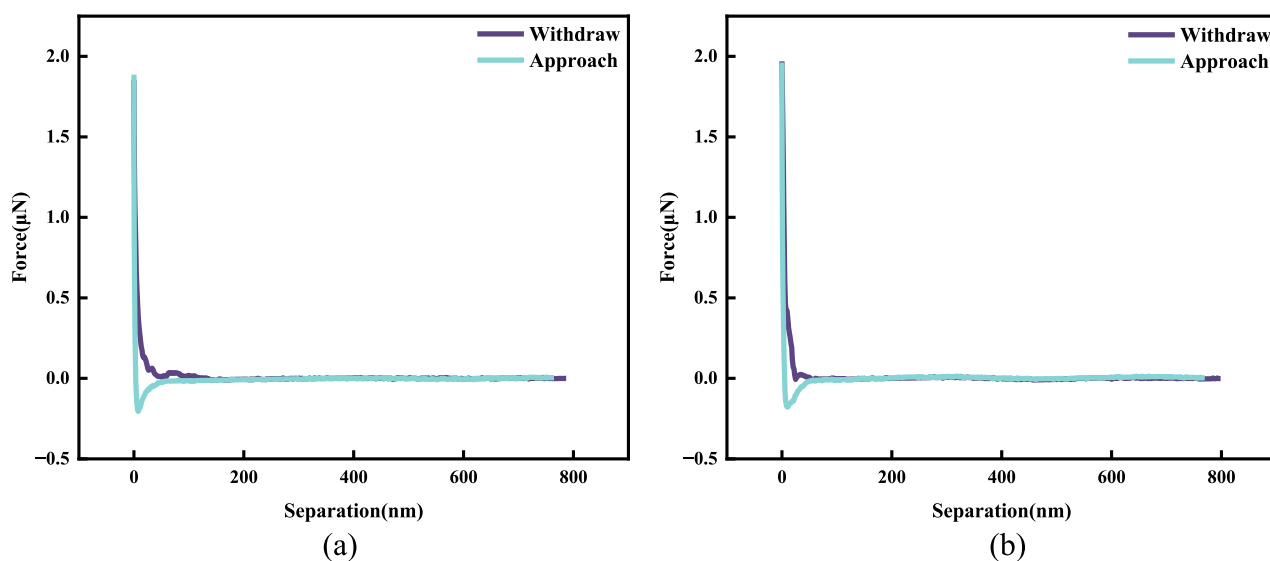


FIGURE 14
Force curve for aggregate. (a) limestone. (b) Granite.

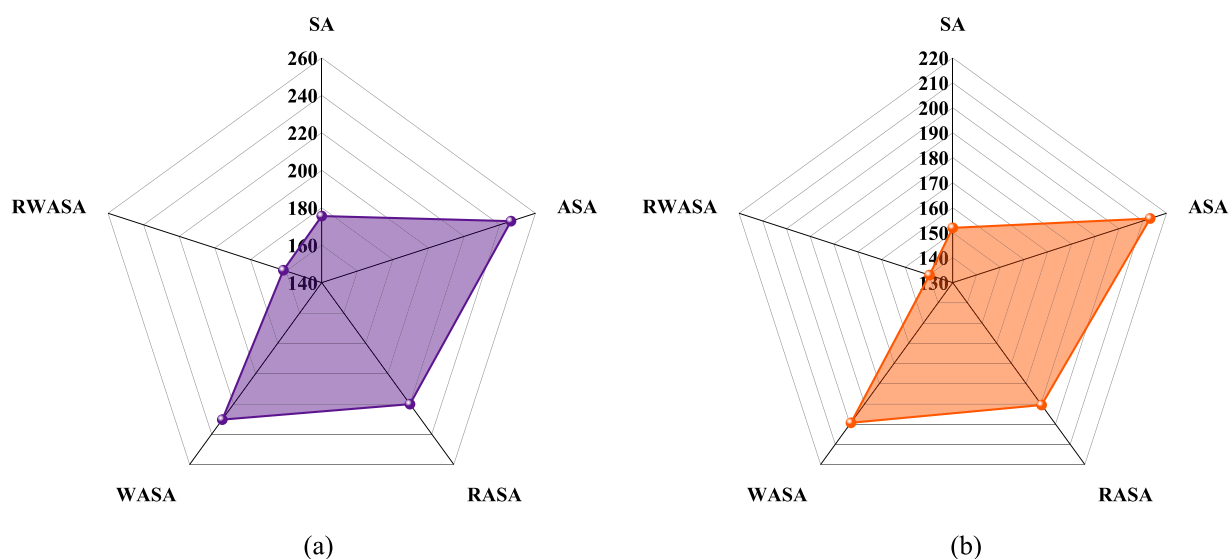


FIGURE 15
Interfacial adhesion work between asphalt and aggregate. (a) limestone. (b) Granite.

The second is because the warm mix agent will crystallize at room temperature, hindering the contact between the polar component and the silicon probe, reducing the adhesion between the asphalt and the silicon probe.

3.1.2 Aggregate micromechanical analysis

This study plotted the force profiles of limestone and Granite, as shown in Figure 14.

Using atomic force microscopy with silicon probes, this study quantitatively characterized the interfacial adhesion properties between asphalt and different mineral aggregates. Experimental data revealed that the limestone-asphalt system exhibited an

interfacial adhesion force of 205.1 nN, significantly higher than the 177.5 nN measured for the granite-asphalt system (representing a 16.6% relative increase). This difference arises mainly from the synergistic effects of interfacial interaction forces, i.e., van der Waals, electrostatic and capillary forces (Pahlavan et al., 2022).

From a materials chemistry point of view, limestone consists mainly of calcite (CaCO_3), while granite consists mainly of silica (SiO_2). This fundamental difference in chemical composition directly leads to their distinct adhesion performance in asphalt systems. The test results not only validate the structure-activity relationship between aggregate chemical composition and

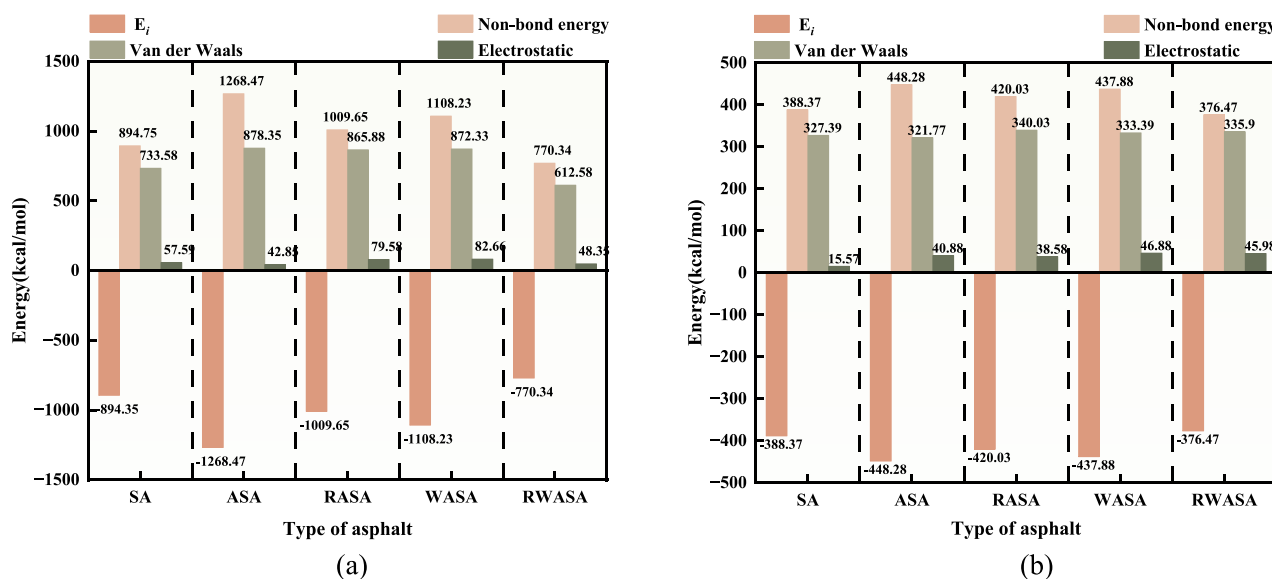


FIGURE 16 Interaction energy between asphalt and oxide mineral. (a) CaCO₃. (b) SiO₂.

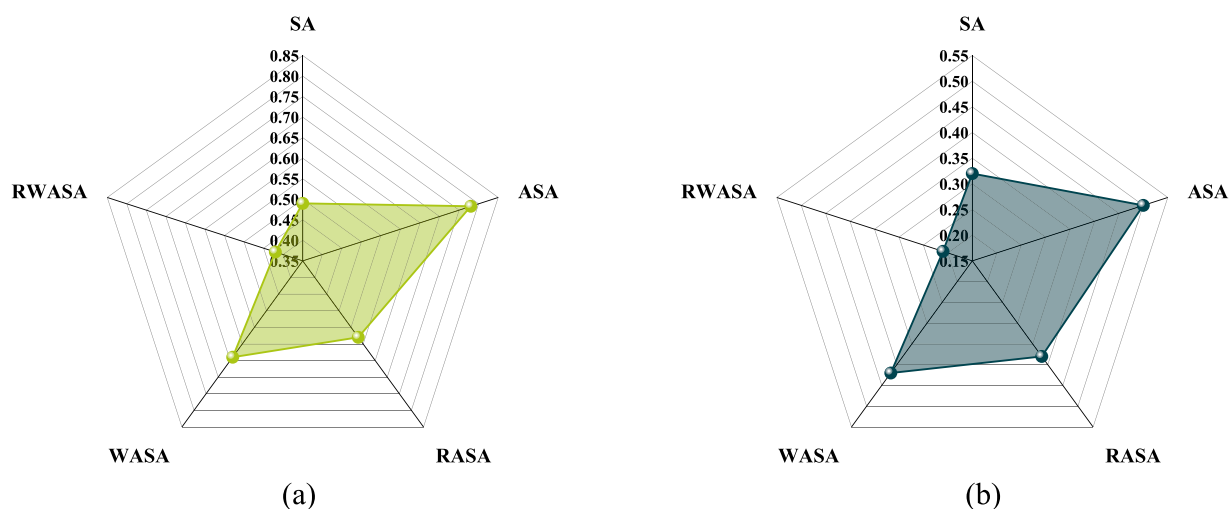


FIGURE 17 Adhesion work of asphalt and oxidized minerals. (a) CaCO₃. (b) SiO₂.

interfacial adhesion, but more importantly, provide theoretical basis for scientific aggregate selection in asphalt mixture design. These findings show strong consistency with existing research conclusions on interfacial behavior of mineral materials (Ji et al., 2020).

3.1.3 Adhesion properties of asphalt-aggregate interface

The data from 3.1.1 to 3.1.2 are brought into Equations 3–5 to obtain the asphalt-aggregate interfacial adhesion work W_{as-ag} , as shown in Figure 15. Figure 15a shows the results of the calculation of the interfacial adhesion work between the five asphalts SA, ASA, RASA, WASA, and RWASA with limestone. Figure 15b shows

the results of the calculation of the interfacial adhesion work between the five asphalts SA, ASA, RASA, WASA, and RWASA with limestone. The interfacial adhesion work between the five asphalts SA, ASA, RASA, WASA, and RWASA and the granite are illustrated in Figure 15b. From Figure 15, it can be seen that the trend of the adhesion work between asphalt and aggregate is consistent with the trend in Section 3.1.1. The mechanistic explanation is also consistent with Section 3.1.1. In addition, it is clear from Figure 15a,b that the adhesion work of asphalt with limestone is much higher than that of asphalt with granite. For example, the work of adhesion of SA to limestone is 175.57 mJ/m², while the work of adhesion of SA to granite is 151.94 mJ/m².

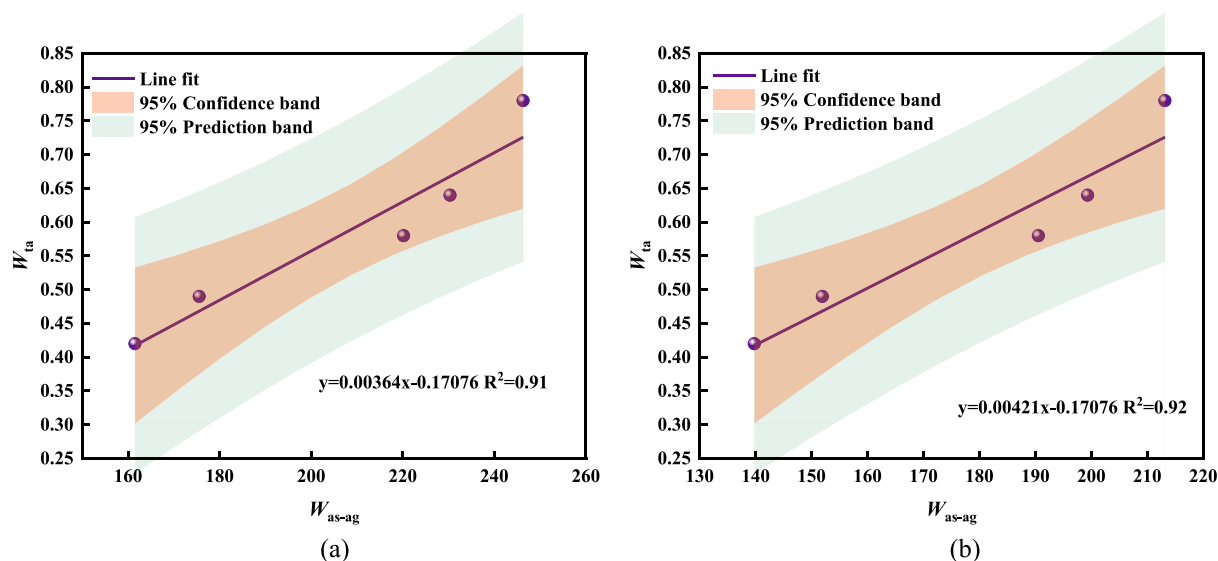


FIGURE 18
The results of linear fitting of AFM and MD. (a) CaCO_3 . (b) SiO_2 .

This result is consistent with the findings of previous studies (Li et al., 2021; Pstrowska et al., 2022; Guo M. et al., 2023). This depends on the chemical composition of the limestone and granite components. The main mineral composition of limestone is CaCO_3 and the main mineral composition of granite is SiO_2 (Cui et al., 2014; Huang et al., 2023). This is due to the fact that CaCO_3 is a negatively charged alkaline oxide, which can generate large interaction forces with positively charged asphalt, resulting in a greater adhesion work between asphalt and limestone than between asphalt and granite (Zhu et al., 2024).

3.2 Molecular dynamics results analysis

3.2.1 Interaction energy

Figure 16 illustrates the interaction energy between bitumen and oxidised minerals. Figure 16a shows the interaction energy between asphalt with CaCO_3 and Figure 16b shows the interaction energy between asphalt with SiO_2 .

As illustrated in Figure 16, the interfacial adhesion between SBS-modified asphalt and aggregates is predominantly governed by non-bonding interactions, with minimal contribution from chemical bonding. This suggests that the primary mechanism of adhesion is physical adsorption, particularly driven by van der Waals forces, rather than chemical reactions. These findings align with prior research (Xu et al., 2023; Yang and Yu, 2023), further supporting the conclusion that intermolecular forces play a decisive role in the asphalt-aggregate bonding behavior.

3.2.2 Adhesion work

In order to gain more insight into the adhesion properties of the asphalt-aggregate interface on a molecular scale, the binding energy was calculated using Equation 7. The results, presented in Figure 17,

reveal key trends in the interaction mechanisms between SBS-modified asphalt and mineral aggregates.

Figure 17 demonstrates a significant enhancement in interfacial adhesion work for aged asphalt-aggregate systems relative to unaged samples, with this trend being consistently observed across different aggregate compositions. The observed improvement principally results from oxidative aging-induced generation of polar functional groups (particularly carbonyl and sulfoxide moieties) (Tang et al., 2024; Yin et al., 2017; Guo et al., 2020), which substantially strengthen both van der Waals forces and electrostatic interactions at the interface, as evidenced in Figure 17. Notably, Figure 17 reveals that asphalt- CaCO_3 systems exhibit significantly stronger interfacial adhesion than asphalt- SiO_2 systems, a result that aligns with existing knowledge in asphalt-aggregate interface science.

The differential adhesion behavior originates from fundamental differences in aggregate surface chemistry (Yin et al., 2017; Guo et al., 2020). While SiO_2 , as an acidic oxide with inherent oleophobicity, forms weaker bonds with asphalt, CaCO_3 's ionic crystal structure—featuring Ca^{2+} cations and CO_3^{2-} anions—creates numerous active surface sites. The Ca^{2+} ions particularly facilitate stronger electrostatic attraction with asphalt molecules, accounting for limestone's superior adhesion performance compared to granite. Moreover, the warm mix agent and rejuvenator altered the adhesion energy between SBS-modified asphalt and aggregate mainly by adjusting the van der Waals forces, as shown in Figure 17. This is due to the fact that the addition of warm mix agent and rejuvenator weakened the interaction energy between the polar functional groups in the aged asphalt and CaCO_3 and SiO_2 .

3.3 Correlation analysis

To further investigate the aging effect, rejuvenator and warm mix on the adhesion mechanism between SBS-modified asphalt

and aggregate, a linear fitting equation between AFM and MD was developed, as shown in Figure 18.

The results in Figure 18 show that there is a significant positive correlation between the interfacial adhesion work calculated by AFM and the adhesion work calculated by MD. The correlation coefficient, $R^2 > 0.9$. In addition, this study confirms the consistency between AFM and MD in evaluating the interfacial state.

4 Conclusion

This study used atomic force microscopy (AFM) to examine the surface microstructure of asphalt and aggregates. The adhesion work between asphalt and aggregate was calculated based on the contact mechanics JKR and DMT models. Molecular dynamics (MD) methods were used to investigate the interaction energy between asphalt and aggregates, and the adhesion work between asphalt and aggregates at the molecular level was calculated. A linear relationship between the AFM and MD scales was established. The main conclusions are as follows:

- (1) Aging causes a significant increase in the number of asphalt columnar structures, which are knots of accumulated polar molecules. Whereas rejuvenators restore the asphalt morphology by supplementing the light component, warm mix agents increase the columnar structure.
- (2) Aging increases asphalt-probe adhesion by 49.96 nN through polar group formation, while rejuvenators and warm-mix additives reduce adhesion by 22.45 nN and 11.27 nN respectively via component replenishment and crystallization effects.
- (3) Compared to the granite-asphalt system, the limestone-asphalt system has a stronger interfacial adhesion, which is a result of the synergistic effect of van der Waals interactions and acid-base electrostatic forces. This trend persists across all asphalt types, validating the dominant role of aggregate mineralogy in adhesion performance.
- (4) The asphalt-aggregate interface is primarily governed by physical adsorption rather than chemical bonding, with aged asphalt showing enhanced adhesion due to oxidative generation of polar groups. Limestone (CaCO_3) exhibits superior adhesion to asphalt compared to granite (SiO_2) because its ionic surface enables stronger electrostatic interactions, while rejuvenators and warm-mix agents modulate adhesion by altering interfacial van der Waals forces.
- (5) The strong positive correlation ($R^2 > 0.9$) between AFM-measured and MD-calculated adhesion work validates both methods for interfacial evaluation, demonstrating their consistency in characterizing asphalt-aggregate interactions.

References

- AASHTO (2024). Standard method of test for effect of heat and air on a moving film of asphalt binder. *Roll. Thin-Film Oven Test*.
- Abd El-Hakim, R. T., Epps, J., Epps Martin, A., and Arámbula-Mercado, E. (2021). Laboratory and field investigation of moisture susceptibility of hot and warm mix asphalts. *Int. J. Pavement Eng.* 22 (11), 1389–1398. doi:10.1080/10298436.2019.1694150
- Ayazi, M. J., Moniri, A., and Barghabany, P. (2017). Moisture susceptibility of warm mixed-reclaimed asphalt pavement containing Sasobit and Zycotherm additives. *Petroleum Sci. Technol.* 35 (9), 890–895. doi:10.1080/10916466.2017.1290655
- Chen, A., Liu, G., Zhao, Y., Li, J., Pan, Y., and Zhou, J. (2018). Research on the aging and rejuvenation mechanisms of asphalt using atomic force microscopy. *Constr. Build. Mater.* 167, 177–184. doi:10.1016/j.conbuildmat.2018.02.008

Data availability statement

The original contributions presented in the study are included in the article/supplementary material, further inquiries can be directed to the corresponding author.

Author contributions

XiW: Writing – original draft. SC: Investigation, Writing – review and editing, Supervision. XuW: Writing – review and editing, Validation. QM: Software, Visualization, Formal Analysis, Writing – review and editing.

Funding

The author(s) declare that no financial support was received for the research and/or publication of this article.

Conflict of interest

Author XW was employed by Gansu Hengda Road and Bridge Engineering Co., Ltd. Author SC was employed by Gansu New Development Investment Group Co., Ltd.

The remaining authors declare that the research was conducted in the absence of any commercial or financial relationships that could be construed as a potential conflict of interest.

Generative AI statement

The author(s) declare that no Generative AI was used in the creation of this manuscript.

Publisher's note

All claims expressed in this article are solely those of the authors and do not necessarily represent those of their affiliated organizations, or those of the publisher, the editors and the reviewers. Any product that may be evaluated in this article, or claim that may be made by its manufacturer, is not guaranteed or endorsed by the publisher.

- Chen, Y., Hou, Y., Ji, X., Zou, H., Dai, C., and Chen, B. (2021). Characterization of surface mechanical properties of various aggregates from micro scale using AFM. *Constr. Build. Mater.* 286, 122847. doi:10.1016/j.conbuildmat.2021.122847
- Cui, B., Gu, X., Wang, H., and Hu, D. (2022). Numerical and experimental evaluation of adhesion properties of asphalt-aggregate interfaces using molecular dynamics simulation and atomic force microscopy. *Road Mater. Pavement Des.* 23 (7), 1564–1584. doi:10.1080/14680629.2021.1910547
- Cui, S., Blackman, B. R., Kinloch, A. J., and Taylor, A. C. (2014). Durability of asphalt mixtures: effect of aggregate type and adhesion promoters. *Int. J. Adhesion Adhesives* 54, 100–111. doi:10.1016/j.ijadhadh.2014.05.009
- Ding, H., Wang, H., Qu, X., Varveri, A., Gao, J., and You, Z. (2021). Towards an understanding of diffusion mechanism of bio-rejuvenators in aged asphalt binder through molecular dynamics simulation. *J. Clean. Prod.* 299, 126927. doi:10.1016/j.jclepro.2021.126927
- Gao, Y., Yu, X., Fan, X., Zhang, H., Xia, Q., Zhou, Z., et al. (2025). Evaluation of adhesion performance and molecular dynamics simulation of SBS-modified asphalt during the field aging. *Constr. Build. Mater.* 474, 141116. doi:10.1016/j.conbuildmat.2025.141116
- Guo, F., Pei, J., Huang, G., Zhang, J., Falchetto, A. C., and Korkiala-Tanttu, L. (2023a). Investigation of the adhesion and debonding behaviors of rubber asphalt and aggregates using molecular dynamics simulation. *Constr. Build. Mater.* 371, 130781. doi:10.1016/j.conbuildmat.2023.130781
- Guo, F., Pei, J., Zhang, J., Xue, B., Sun, G., and Li, R. (2020). Study on the adhesion property between asphalt binder and aggregate: a state-of-the-art review. *Constr. Build. Mater.* 256, 119474. doi:10.1016/j.conbuildmat.2020.119474
- Guo, M., Yin, X., Du, X., and Tan, Y. (2023b). Effect of aging, testing temperature and relative humidity on adhesion between asphalt binder and mineral aggregate. *Constr. Build. Mater.* 363, 129775. doi:10.1016/j.conbuildmat.2022.129775
- Han, J., Li, B., Ji, H., Guo, F., Wei, D., Cao, S., et al. (2024). Interfacial adhesion between recycled asphalt binder and aggregates considering aggregate surface anisotropy: a molecular dynamics simulation. *Constr. Build. Mater.* 438, 137176. doi:10.1016/j.conbuildmat.2024.137176
- Hu, Y., Si, W., Kang, X., Xue, Y., Wang, H., Parry, T., et al. (2022). State of the art: multiscale evaluation of bitumen ageing behaviour. *Fuel* 326, 125045. doi:10.1016/j.fuel.2022.125045
- Hu, Y., Xia, W., Xue, Y., Zhao, P., Wen, X., Si, W., et al. (2023). Evaluating the ageing degrees of bitumen by rheological and chemical indices. *Road Mater. Pavement Des.* 24 (Suppl. 1), 19–36. doi:10.1080/14680629.2023.2180289
- Huang, G., Zhang, J., Wang, Z., Guo, F., Li, Y., Wang, L., et al. (2023). Evaluation of asphalt-aggregate adhesive property and its correlation with the interaction behavior. *Constr. Build. Mater.* 374, 130909. doi:10.1016/j.conbuildmat.2023.130909
- Ji, H., Li, B., Yao, T., Liu, Z., Han, J., and Li, A. (2023). Polyurethane and nano-TiO₂ modifiers mitigate aging of asphalt binders by inhibiting aggregation of polar molecules: a molecular dynamics study. *Colloids Surfaces A Physicochem. Eng. Aspects* 679, 132654. doi:10.1016/j.colsurfa.2023.132654
- Ji, X., Sun, E., Zou, H., Hou, Y., and Chen, B. (2020). Study on the multiscale adhesive properties between asphalt and aggregate. *Constr. Build. Mater.* 249, 118693. doi:10.1016/j.conbuildmat.2020.118693
- Li, D. D., and Greenfield, M. L. (2014). Chemical compositions of improved model asphalt systems for molecular simulations. *Fuel* 115, 347–356. doi:10.1016/j.fuel.2013.07.012
- Li, J., Wang, Z., and Jia, M. (2021). Comprehensive analysis on influences of aggregate, asphalt and moisture on interfacial adhesion of aggregate-asphalt system. *J. Adhesion Sci. Technol.* 35 (6), 641–662. doi:10.1080/01694243.2020.1816792
- Li, Q., Wang, J., Song, S., Wang, R., Jiang, J., and Yan, C. (2023). Study on the adhesion characteristics of asphalt-aggregate interface in cold recycled asphalt mixtures. *J. Mater. Civ. Eng.* 35 (9), 04023283. doi:10.1061/JMCEE7.MTENG-15572
- Liu, S., Zhang, E., Shan, L., and Li, G. (2025). Molecular mechanisms of interfacial adhesion between asphalt and mineral aggregates based on molecular dynamics and density functional theory. *Transp. Res. Rec.*, 03611981251328981. doi:10.1177/0361198125132898
- Luan, Y., Ma, T., Wang, S., Ma, Y., Xu, G., and Wu, M. (2022). Investigating mechanical performance and interface characteristics of cold recycled mixture: promoting sustainable utilization of reclaimed asphalt pavement. *J. Clean. Prod.* 369, 133366. doi:10.1016/j.jclepro.2022.133366
- Ma, X., Wang, D., Liu, S., Jiang, J., Kan, J., and Tu, M. (2024). Analysis of asphalt microscopic and force curves under water-temperature coupling with AFM. *Case Stud. Constr. Mater.* 20, e03071. doi:10.1016/j.cscm.2024.e03071
- Mohammed, S. F., and Ismael, M. Q. (2021). Effect of polypropylene fibers on moisture susceptibility of warm mix asphalt. *Civ. Eng. J.* 7 (6), 988–997. doi:10.28991/cej-2021-03091704
- Pahlavan, F., Lamanna, A., Park, K.-B., Kabir, S. F., Kim, J.-S., and Fini, E. H. (2022). Phenol-rich bio-oils as free-radical scavengers to hinder oxidative aging in asphalt binder. *Resour. Conservation Recycl.* 187, 106601. doi:10.1016/j.resconrec.2022.106601
- Pan, Y., Han, D., Yang, T., Tang, D., Huang, Y., Tang, N., et al. (2021). Field observations and laboratory evaluations of asphalt pavement maintenance using hot in-place recycling. *Constr. Build. Mater.* 271, 121864. doi:10.1016/j.conbuildmat.2020.121864
- Pstrowska, K., Gunka, V., Sidun, I., Demchuk, Y., Vytrykush, N., Kulażyński, M., et al. (2022). Adhesion in bitumen/aggregate system: adhesion mechanism and test methods. *Coatings* 12 (12), 1934. doi:10.3390/coatings12121934
- Qu, X., Liu, Q., Guo, M., Wang, D., and Oeser, M. (2018). Study on the effect of aging on physical properties of asphalt binder from a microscale perspective. *Constr. Build. Mater.* 187, 718–729. doi:10.1016/j.conbuildmat.2018.07.188
- Sun, E., Zhao, Y., and Cai, R. (2024). Characterization of microstructural evolution of asphalt due to water damage using atomic force microscopy. *Constr. Build. Mater.* 438, 137175. doi:10.1016/j.conbuildmat.2024.137175
- Sun, G., Zhang, J., Niu, Z., Huang, Y., Shi, P., and Zhang, S. (2025). Characterization of physicochemical composition of asphalt/aggregate and multi-scale analysis of interfacial adhesion behavior. *Mater. Struct.* 58 (2), 64–21. doi:10.1617/s11527-025-02592-2
- Tang, Y., Fu, Z., Ma, F., Hou, Y., and Zhao, P. (2024). Molecular dynamics simulation on asphalt-limestone interfaces considering unconstrained surfaces and individual colloid components. *Constr. Build. Mater.* 424, 135923. doi:10.1016/j.conbuildmat.2024.135923
- Wang, J., Li, Q., Lu, Y., and Luo, S. (2022). Effect of Waste-Oil regenerant on diffusion and fusion behaviors of asphalt recycling using molecular dynamics simulation. *Constr. Build. Mater.* 343, 128043. doi:10.1016/j.conbuildmat.2022.128043
- Wang, W., Huang, S., Qin, Y., Sun, Y., and Chen, J. (2020). Multi-scale study on the high percentage warm-mix recycled asphalt binder based on chemical experiments. *Constr. Build. Mater.* 252, 119124. doi:10.1016/j.conbuildmat.2020.119124
- Xie, H., Liu, Y., Long, Z., Xu, F., You, L., Tang, X., et al. (2023). Micro-characterization of the adhesion properties and mechanisms at the asphalt-silica aggregate interface under combined thermal-oxygen aging and chloride salt erosion. *Constr. Build. Mater.* 401, 132818. doi:10.1016/j.conbuildmat.2023.132818
- Xu, Z., Zhang, J., Jing, Y., Huang, G., He, H., and He, Y. (2023). Research on the evolution of adsorption behavior of asphalt and aggregate surface and its influencing factors. *Case Stud. Constr. Mater.* 19, e02500. doi:10.1016/j.cscm.2023.e02500
- Yang, Q., and Yu, C. (2023). Deterioration effects of oxidative aging on graphene-asphalt nanocomposite interfaces: multiscale Modeling. *Langmuir* 39 (23), 8339–8353. doi:10.1021/acs.langmuir.3c00917
- Yin, Y., Chen, H., Kuang, D., Song, L., and Wang, L. (2017). Effect of chemical composition of aggregate on interfacial adhesion property between aggregate and asphalt. *Constr. Build. Mater.* 146, 231–237. doi:10.1016/j.conbuildmat.2017.04.061
- Yu, H., Ge, J., Qian, G., Shi, C., Zhang, C., Dai, W., et al. (2023b). Evaluation of the interface adhesion mechanism between SBS asphalt and aggregates under UV aging through molecular dynamics. *Constr. Build. Mater.* 409, 133995. doi:10.1016/j.conbuildmat.2023.133995
- Yu, H., Ge, J., Qian, G., Zhang, C., Dai, W., and Li, P. (2023a). Evaluation on the rejuvenation and diffusion characteristics of waste cooking oil on aged SBS asphalt based on molecular dynamics method. *J. Clean. Prod.* 406, 136998. doi:10.1016/j.jclepro.2023.136998
- Yu, T., Wang, J., Zhang, H., and Sun, J. (2024). Microanalysis of behavior characteristics for asphalt binders on different mineral surfaces based on MD and SEM. *Constr. Build. Mater.* 438, 137292. doi:10.1016/j.conbuildmat.2024.137292
- Zhang, D., Zheng, Y., Yuan, G., Zhang, Y., Qian, G., and Zhang, H. (2022a). Research on the field aging gradient behavior of SBS-modified bitumen at different depths of pavement by rheological and microscopic characterization. *Fuel* 329, 125192. doi:10.1016/j.fuel.2022.125192
- Zhang, E., Shan, L., Qi, X., Wang, X., and Fan, Y. (2022b). Investigating the relationship between chemical composition and mechanical properties of asphalt binders using atomic force microscopy (AFM). *Constr. Build. Mater.* 343, 128001. doi:10.1016/j.conbuildmat.2022.128001
- Zhang, M., Wang, Y., Zhang, W., Du, W., Li, X., Wang, X., et al. (2024a). Adhesion characteristics of montmorillonite modified asphalt unveiled by surface free energy and AFM. *Int. J. Adhesion Adhesives* 132, 103699. doi:10.1016/j.ijadhadh.2024.103699
- Zhang, Z., Jun, Z., Gu, R., Fu, J., He, C., and Chen, X. (2024b). Effect of aging on micromechanical behavior of asphalt surfaces using an atomic force microscopy. *Case Stud. Constr. Mater.* 20, e03098. doi:10.1016/j.cscm.2024.e03098
- Zhu, S., Kong, L., Peng, Y., Chen, Y., Zhao, T., Jian, O., et al. (2024). Mechanisms of interface electrostatic potential induced asphalt-aggregate adhesion. *Constr. Build. Mater.* 438, 137255. doi:10.1016/j.conbuildmat.2024.137255